

**Lightweight Cellular Concrete as a Subbase Alternative in Pavements: Instrumentation plan,
Installation and Preliminary results**

Abimbola Grace Oyeyi, Ph.D. Candidate, Department of Civil and Environmental Engineering
University of Waterloo

Frank Mi-Way Ni, Ph.D. Candidate, Department of Civil and Environmental Engineering
University of Waterloo

Dr. Daniel Pickel, Research Associate, Department of Civil and Environmental Engineering
University of Waterloo

Dr. Susan L. Tighe, Deputy Provost and Associate Vice-President Integrated Planning and
Budgeting, Norman W. McLeod Professor in Sustainable Pavement Engineering, Department of
Civil and Environmental Engineering, University of Waterloo

Paper prepared for presentation at the Innovations in Pavement Management, Engineering and
Technologies Session of the 2019 TAC-ITS Canada Joint Conference, Halifax, NS

Acknowledgments:

The authors will like to thank the Region of Waterloo, CEMATRIX Canada, Steed and Evans, and
the Centre for Pavement and Transportation Technology (CPATT), University of Waterloo, for
supporting this research. Funding for this research is in part provided by CEMATRIX Canada and
Natural Sciences and Engineering Association of Canada (NSERC)

Abstract

The use of Lightweight Cellular Concrete (LCC) in the pavement structure is a potential solution to reducing the burden of the pavement on the roadbed, especially over weak soils, hence alleviating potential rutting and other forms of distress. Evaluating the performance feasibility of such materials is necessary, especially in comparison to traditional materials. This will involve both field and laboratory evaluation to provide relevant information for its application. As part of the field evaluation, a design that incorporated LCC as a subbase alternative in the pavement structure was developed and constructed. A shoulder bus stop which experienced severe rutting and cracking was selected as a trial location. The design of the trial included one control section constituting Granular B as subbase material and two LCC sections with LCC thicknesses of 250mm and 350mm as subbase material. Subsurface instrumentation was installed in each layer of the three sections including strain gauges, pressure cells, moisture probes, maturity sensors, and temperature strings. A weather station consisting of a rain gauge and solar radiation shield was also installed at the location of the trial section to monitor weather events. The instrumentation has been monitored to obtain information about the trial section with LCC and compare with the traditional Granular B material. Readings from the maturity sensors indicated that the concrete hydration process peaked at about twelve hours for both LCC sections and depicted a 28-day compressive strength of 1.67MPa and an ultimate strength estimated to reach 2.20MPa and 2.02MPa for the LCC 350 and 250 sections respectively. Temperature profiles indicated higher temperatures within and below the LCC layers compared to the control section, portraying LCC insulation properties. Moisture conditions were generally found to be saturated for all layers in all section during the preliminary study period. In general, data from all installed sensors including pressure cells and strain gauges, in addition to results already discussed are presented in this paper.

1.0 Introduction

Enhancing the long-term performance of road infrastructure is an essential goal for engineers in Canada, especially with changing climatic conditions. This has brought about varying approaches in design and construction techniques with alternative materials. Also, due to severe climatic conditions with frost and rapid temperature variations, weaker and frost-susceptible subgrades are produced (Hoff et al., 2002) as is the case for Canada. Frequently, Canadian roads and highways are constructed over weak subgrades consisting of peat, organics or soft soil deposits which cause them to undergo continual and long term settlements (Maher and Hagan, 2016). These roads usually require frequent patch repairs which in turn could lead to even more settlements due to additional loading to the pavement structure. Traditional full-depth reconstruction to remove compressible layers can be costly, especially for depths greater than one meter. Full depth reconstruction is also disruptive to road users, and not sustainable due to the production of large quantities of excess materials and the use of virgin material (Maher and Hagan, 2016).

To mitigate the problem of weaker subgrades, improving the subbase layer with new materials should be considered. As the subbase is a significant part of the pavement structure which helps

in transmitting loading from upper layers to the subgrade, significant innovations in subbase material composition are necessary. Traditionally, the unbound crushed stone material is utilized to perform these functions. However, since it is made of virgin material, it contributes to the depletion of natural resources and constitutes additional environmental hazards due to its production, transportation and the increased cost incurred. The material also contributes to the settlement problem as its weight is a burden to the subgrade (Mallick and El-Korchi, 2013).

Lightweight materials that have the potential to reduce settlements and bearing failures are being researched. Lightweight Cellular Concrete (LCC) is one such material. LCC, also known as foamed concrete, foam concrete or reduced density concrete, contains cement slurry, foam and compressed air which influences its light weight (Dolton et al. 2016). The use of LCC dates back to the early nineteenth century, however in-depth studies about the material composition, physical properties, and production was only carried out in the 1950s (Valore, 1954a). Since then, there has been ongoing research on how to improve its characteristics and applications.

LCC applications have evolved over the years from void fillings to ground stabilization and more recently as a structural component in the infrastructure. Because LCC has a wide range of density, typically 250 to 1,600 kg/m³, it gives the flexibility that could enable its use in numerous applications (Concrete Society, 2009; Narayanan and Ramamurthy, 2000). Specifically, it has been used for filling large voids, floor screeding, insulating foundations thermally, strengthening bridges, backfilling and as pre-cast blocks (Ozlutas, 2015). Also, it has been used for soil stabilization, pipe beddings, sound walls, and insulation, filling abandoned pipes, tanks, and mines and as arrester material at the end of the runway which crushes and stops overshooting aircraft (Dolton et al., 2016; Horpibulsuk et al., 2014).

The use of LCC as part of the pavement structure is also gaining recognition especially in areas with weaker subgrades. Many such applications in Canada have been undertaken, including bus lanes in Calgary, Alberta, and Caledon, Ontario, mostly to solve settlement problems due to weak subgrades (Maher and Hagan, 2016; Dolton et al., 2016). With LCC applications and previous studies, there is still limited information and guidelines for its use in the pavement structure. Previous studies have mainly concentrated on mechanical properties via laboratory testing; however, there is no comprehensive field performance data for its application in road construction.

2.0 Objective and Scope

A field investigation which involves a trial section could give significant opportunity to explore the application of LCC in the pavement structure and understand how it behaves and will perform, under varying conditions. This understanding will help explain performance throughout its lifespan and contribute to the development of guidelines for its use. A thorough understanding of the use of LCC in the pavement structure is required to explore the possibility of future applications by understanding factors influencing its performance. To this effect, part of the investigation outlined in this paper included the placement of instrumentation within the pavement layers. This paper aims to describe the instrumentation installation procedure and

present preliminary information obtained from the instrumentation. Results will help identify potential factors that could impact the performance of the pavement with LCC in comparison to the traditional Granular B pavement structure. The LCC material in this study consists of 80% cement, 20% slag and a cementitious/water ratio of 0.5. Asphalt concrete, Granular A and Granular B material were following the Ontario Provincial standard for roads and public works (OPSS).

2.1 Project location and Instrumentation

The trial section is located on the southbound shoulder section of a two-lane arterial road at the intersection of Erbsville Road and Brandenburg Blvd, in Waterloo, Ontario. The geographic Cartesian coordinates of the site are 43°27'34.6"N 80°34'42.3"W. This shoulder also serves as a bus stop and is selected by the Region of Waterloo as a trial location as it experienced severe cracking and rutting issues, as seen in Figure 1. The cause of these distresses is uncertain, but it might be a weak subgrade. The trial section was 40m long, beginning at the intersection. The section of the roadway was relatively flat and straight.



Figure 1: Distress at Bus stop

A part of obtaining information about the use of LCC in the pavement structure is instrumenting a trial section in addition to post construction testing. Since this application is quite new in Canada, continuous information gathering is required. Post-construction monitoring is on-going and involves roughness measurements, visual inspection, static load testing, and Lightweight and Falling Weight deflectometer testing. Sub-surface instrumentation was installed in each layer of the pavement structure. The section view of the trial project is presented in Figure 2. The design was made up of three sections. All sections have similar upper layer materials and thicknesses: an asphalt concrete surface layer and Granular A base layer. The control section is 10m long and consists of 450mm thick Granular B material as subbase. The other two sections include LCC subbase layers of 350mm and 250mm thickness. These sections are referred to as LCC 350 and LCC 250, respectively. Each LCC section is 15m long.

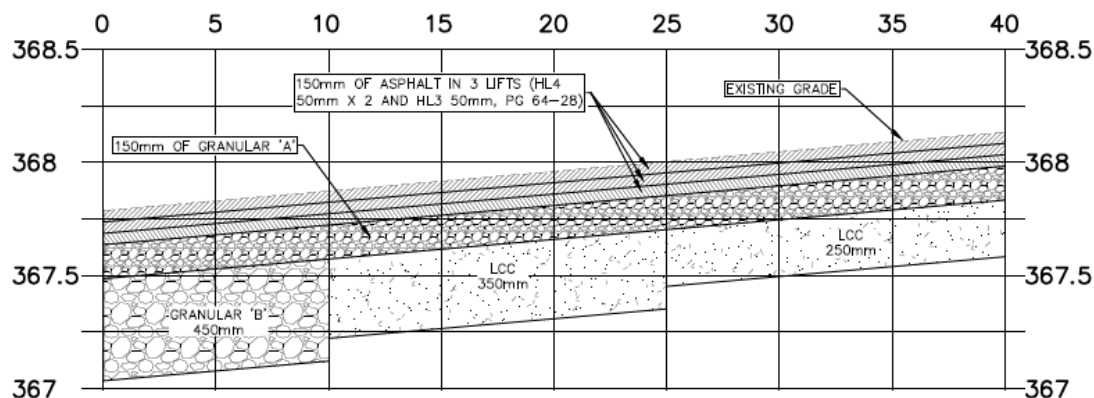


Figure 2: Section view of the trial section

Five types of sensors were installed within the pavement structure. The sensors included strain gauges, moisture sensors, temperature strings, earth pressure cells, and maturity sensors. Two additional sensors were installed beside the roadway to measure the environment. A summary of all the sensors installed, model and quantity are presented in Table 1.

Table 1: Sensor summary

Sensor type	Model	Number installed	Measurements made	Sampling frequency (readings/hour)
Earth pressure cell	LPTPC09-V	3	VW frequency (Hz) Thermistor resistance (ohm)	12
Maturity sensor (Command center)	301006-X85	2	Temperature-Time Factor (TTF-hr) Temperature (°C) Ultimate strength (MPa)	2
Strain gauge	ASG 152	14	μ strain mV/V	12
Thermistor string	T107 series	3 strings (7 sensors each)	Temperature (°C)	12
Moisture probe	Watermark 200SS	9	Thermistor resistance (ohm) Water potential (CB or KPa)	12
Rain gauge	NovaLynx 260-2500	1	Precipitation (mm)	2
Solar radiation shield/Temperature data logger	Hobo pendant UA-003-36	1	Temperature (°C)	2

Information obtained from the sensors included that relating to the presence of moisture within the layers and moisture movement from the top layers down. Moisture sensors were placed in the base, subbase, and subgrade layers for all sections to monitor this.

Information on the temperature profile within the pavement structure for each section was measured using thermistor strings. Strain levels within the pavement layers are also crucial to the long-term performance of the pavement. Strain gauges were placed at the bottom of the asphalt layer to monitor tensile strain, which is linked to fatigue performance. Strain gauges were also installed at the middle and bottom of the LCC layers to measure the strains within the

subbase layer. Information on the setting time of LCC was obtained using concrete maturity meters which were placed in the middle of the LCC layer.

A weather station comprising of a rain gauge and solar radiation shield with a temperature data logger was also installed at the location to monitor weather events and serve as a reference point in interpreting pavement data obtained from sensors.

3.0 Methodology

3.1 Instrumentation Installation

Instrumentation installation coincided with the construction process with each instrument mounted before the construction of the layer where applicable. Construction commenced on the 22nd of October 2018, with excavation and Granular B placement for the control section. LCC placement occurred the next day. Road construction activities ended with asphalt concrete paving on the 5th of November, 2018. A detailed section view showing the type and location of each sensor is given in Figure 3. All sensors were installed beneath the right wheel path of the bus stop.

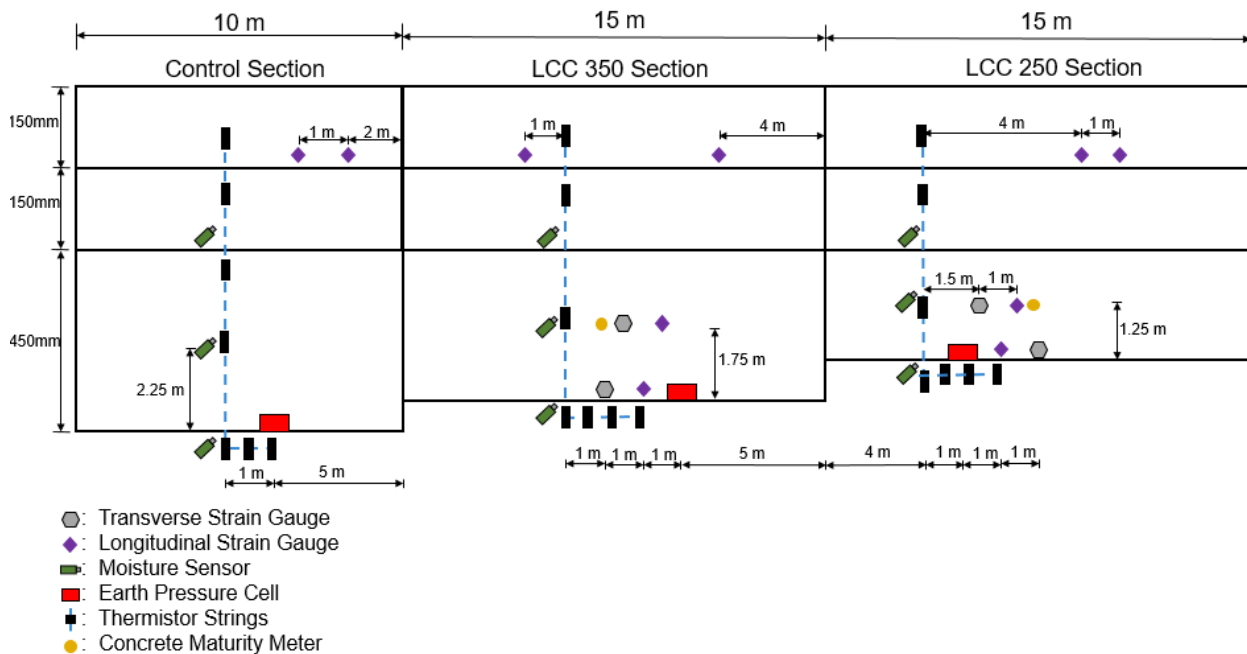


Figure 3: Location of sensors within pavement (section view)

The moisture sensors and temperature strings were installed as one unit for each of the sections. Three moisture sensors and one thermistor string with seven temperature sensors were attached to a tree made of $\frac{3}{4}$ " diameter PVC pipes. A hole was dug in the subgrade soil to receive the moisture tree which was hammered into the subgrade to ensure that at least one moisture and temperature sensor was located in each layer. One moisture sensor was located in the subgrade, the other at the center of the subbase layer and the third at the center of the base layer. The moisture sensors were placed at an angle (more vertically inclined) to ensure they were at the

exact positions intended and they read correctly. Also, at least one temperature sensor was located in each pavement layer including the asphalt layer.

One earth pressure cell was installed in each section. Fine sand obtained offsite was used as the bedding material for the circular head of the cell, with the cell installed on the sand. The cell was held firmly to the ground using metal pegs.

Four strain gauges were placed in the subbase layer for each of the LCC sections, while two each were placed at the bottom of the asphalt layer for all the sections. For the two strain gauges installed at the bottom of the LCC layers, metal pegs were used to firmly fix them in position to the ground surface to ensure no movement during the LCC pour. One strain gauge installed horizontally, while the other was installed in the transverse direction. For strain gauges installed at the middle of the LCC, props to hold them made with $\frac{3}{4}$ " diameter PVC pipes were utilized. Similar to the gauges placed at the bottom of the LCC layer, one was placed in the horizontal direction and the other in the transverse direction.

Concrete maturity meters were also attached to the props used for the mid-LCC strain gauges to ensure that they were located at the mid-point of the LCC layer. The strain gauges in the asphalt layer were placed by digging up the first two lifts of asphalt concrete immediately after it was placed (in one pour) to expose the surface of the base layer. The removed asphalt concrete was replaced to cover up the strain gauge after installing and compacted. The instrumentation cluster is shown in Figure 4a.

All the cabling for the sensors were run in PVC flexible conduit pipes to the side of the excavation and transitioned into a 4" diameter solid PVC pipe which was laid in a trench, dug to meet the data logging unit. The trench pipe ran into a 750mm x 750mm concrete base that held the traffic box with instruments to read the sensors as shown in Figure 4b. The data-logging unit consists of a battery, one 1000V data logger and four multiplexers. The temperature sensors, moisture sensors, strain gauges, and pressure cells are each connected to separate multiplexers. A vibrating wire analyzer is used with the multiplexer for the pressure cell to enable its readings. These logging units are all attached to a plywood board and firmly fixed to the data-logging box.

The construction took place during low temperatures (average of 4°C) and scattered rainfall. This affected the project duration by impeding the placement of Granular A beyond 24 hours after LCC pour. Also, the presence of rainfall resulted in construction activities including the asphalt concrete paving being postponed. It should also be noted that most of the instrumentation was installed during rainy conditions. This might lead to the damage of some sensors. Some technical issues were also encountered in trying to read some measurements from the sensors using the data logger. The measurement methods for each sensor is discussed subsequently.



(a) A cluster of sensors installed

(b) Data-logging unit and weather station

Figure 4: Overall instrumentation

3.2 Moisture Sensors

Moisture was monitored in conjunction with local precipitation information gathered from the weather station installed at the location. Data from this weather station was validated by comparing with two other weather stations. The first of these was the University of Waterloo (UW) weather station with Cartesian coordinates of 43° 28' 25.6" N and 80° 33' 27.5" W and an elevation of 334.4m. It is about 3.8 km by road from the on-site weather station. The second weather station is owned by Environment Canada and is located at the Region of Waterloo International Airport in Breslau, Ontario with Cartesian coordinates of 43° 27' 39.0" N and 80° 22' 43.0" W and is located 24.5 km away from the site.

The moisture sensors included in this trial section are typically used for agricultural applications. They have been selected for use in this research because they can record measurements when not totally surrounded by soil. LCC and granular material have several voids which could mean air being adjacent to the moisture sensors in specific locations. In order to read these sensors, a CR1000 data logger is used. A program was developed to record the moisture measurements of the materials surrounding the sensors. An excitation voltage is sent from the CR1000 to the moisture sensors; a voltage is measured after a pause of three milliseconds. The CR1000 records the measured voltage divided by the excitation voltage which is then converted to resistance and adjusted to 21°C using Equation 1 for a uniform basis of comparison. After this, the resistance is converted to Soil Water Potential (SWP) in centibars (cb) units which is equivalent to KPa via Equation 2 (Henderson, 2012).

$$R_{21} = \frac{R_m}{(0.018(T_m - 21))} \quad (1)$$

Where,

R_{21} is the resistance adjusted to 21°C.

R_m is the resistance reading determined from the raw data collected by the CR1000, in k Ω .

T_m is the temperature of the soil surrounding the moisture gauge in °C.

$$SWP = 7.407 \times R_{21} - 3.704 \quad (2)$$

Where,

SWP is the soil water potential measured in centibars (cb).

SWP (or Tension) describes the availability of water. When water is readily available, the centibar values are closer to zero with a zero value signifying fully saturated, but when minimal water is available, the values become higher (Henderson, 2012). Temperature readings used in conjunction with the moisture sensors were obtained from the thermistor strings installed. The temperature sensor readings used corresponded to those in the same layer as the moisture sensors. Temperature and moisture readings were collected at the same time every five minutes.

3.3 Thermistor strings

Thermistor strings, which consist of seven temperature sensors, were included in the field section to provide subsurface information of temperature variation at different elevations within the pavement structure. Hence, it would enable a comparison of pavement and atmospheric temperature, temperature profile using LCC and Granular B materials, and for use in analyzing the moisture sensor data. The temperature sensors for each string are connected to the CR1000 data logger through one single-ended input channel and a voltage excitation channel with measurements taken by the thermistors within each sensor every five minutes. To obtain accurate readings, temperature sensors must be fully surrounded by material; thus temperature sensors have been embedded close to the mid-point of each layer of the pavement. The daily average temperature value is obtained over a twenty-four hour period. The daily maximum and minimum temperatures are also recorded. The thermistor is designed to resist heat, and the wire is waterproof, which increases the durability of the instrument.

3.4 Pressure cells

The earth pressure cells consist of two circular steel plates welded together around the periphery with the space between the two plates filled with hydraulic fluid. The cell is connected via a stainless steel tube to a transducer forming a closed hydraulic system (El-Hakim, 2009). As the weight of a vehicle is applied on the pavement surface layer through its tires (axle load), vertical stresses in the layer are generated which could lead to rutting. When the stress compresses the cell, the pressure can be measured and transformed into an electric signal. The earth pressure cell consists of a 3 K Ω thermistor that calculates the pressure readings based on the cell fluid viscosity characteristics (Pickel et.al, 2018). These are connected to the CR1000 data logger via a vibrating wire analyzer with measurements taken every five minutes using the program developed.

3.5 Concrete maturity meter

In order to determine the maturity curve using the maturity method, the temperature within the LCC needs to be correlated with its compressive strength over 28 days. To do this, one maturity sensor was installed in the middle of a 150 x 300mm cylindrical specimen taken to the laboratory from the field. This specimen was left undisturbed in the field for twenty-four hours before movement, to avoid changing the structure of the material. At the CPATT laboratory, it was demolded on the seventh day and put in the humidity chamber at 85% humidity. The recorded temperature from the sensor in the specimen was correlated with compressive strength results obtained in the laboratory. The Maturity curve is determined based on strength and Temperature-Time Factor (TTF).

Compressive strength test was performed in accordance with ASTM C495, and C796 on 75 x 150 mm specimen obtained the same time as the specimen with the maturity meter installed. These specimens were tested at 1, 3, 7, 14 and 28 days using a stress-controlled set up. Similar to the maturity meter specimen, they were left undisturbed for twenty-four hours before movement. On day one, four specimens were tested. Before testing, they were demolded and grinded. To calculate the UCS the following equation was used.

$$UCS = \frac{P}{A} \quad (3)$$

where:

UCS = unconfined compressive strength, MPa

P = maximum load recorded, kN

A = the cross-sectional area of the specimen, mm²

Day three specimens were demolded the same day as testing. Four specimens were prepared by grinding their surfaces and tested. On day seven, all the specimens were demolded and placed in the humidity chamber at 85% humidity. The four specimens to be tested on day seven, however, were demolded on day six before testing. Day fourteen specimens were removed from the humidity chamber the morning of the testing. Day twenty-eight specimens were left in the humidity chamber for eighteen days, and air dried afterward for three days before testing.

3.6 Strain gauges

The program developed to record strain measurements of the materials surrounding the sensors included the CR1000 applying an excitation voltage to the full bridge strain gauge installed in the pavement. It then performs strain calculations on the measurement. The resulting value is the measured voltage in units of microstrain (Campbell Scientific, 2005). The installed strain gauge has a nominal resistance of 350 Ω.

4.0 Results

4.1 Moisture

To validate the data from the weather station installed at the location, a two-sample T-test was performed on precipitation data obtained from the site and the UW stations. Results found precipitation readings to be statistically the same with a p-value of 0.99 (> 0.05) at 95% confidence level. Similarly, site and Environment Canada weather station data were found to be statistically the same with a p-value of 0.65.

Figure 5a, b, c shows the moisture tree data for all the section and Figure 5d precipitation data at the location. Lower centibar (cb) values indicate the presence of moisture with zero indicating saturation, while higher values show lower levels or an absence of water. For all sections from November 2018 to March, 2019, indications are that most layers are saturated with water. Considering that these are the winter months, this seems reasonable as the sensors could constantly be sensing water around them. It was observed in late-January that some layers especially the base layer for all sections indicated lower water levels. This period coincides with the highest rainfall recorded during the study period. This could be as a result of the melting of frozen water within the layer and draining away from the base layer. To better understand the moisture characteristics for each section, more data periods in varying weather conditions is needed.

4.2 Temperature

T-test was also performed with temperatures from the UW station to confirm the Erbsville weather station atmospheric temperature readings. Results showed readings to be statistically the same with a p-value of 0.94 (>0.05) at a 95% confidence level. The temperature profile trend within the layers compared with the ambient temperature are presented in Figure 6. It should be noted that due to some technical challenges with reading the temperature data from the LCC 250 thermistor string, it is not included in this analysis. Also, the temperature sensor installed in the surface layer for the LCC 350 is used to show the general pavement surface temperature for all the sections. It was observed that the temperature sensor installed in the surface layer for the control section gave similar readings like the one installed in the base layer. It is possible the sensor was compacted into the base layer during construction so would not read the surface temperature.

The control section subgrade and overall surface layer temperature were discovered to follow a similar trend as the ambient temperature. Regression analysis performed to assess this relationship exhibited R^2 values above 0.5 for these layers (Table 2). It should be noted that other factors such as moisture could also influence subgrade temperature and this should be assessed. However, the trend in the subgrade layer for the LCC sections did not seem to be significantly affected by ambient temperature. Temperatures within the layer remained positive and showed little fluctuations. Similarly, the LCC subbase layer temperatures did not appear to vary with

ambient temperature. This is also the case for the subbase layer of the control section and base layers for all sections, although they had lower temperature readings than the LCC layer.

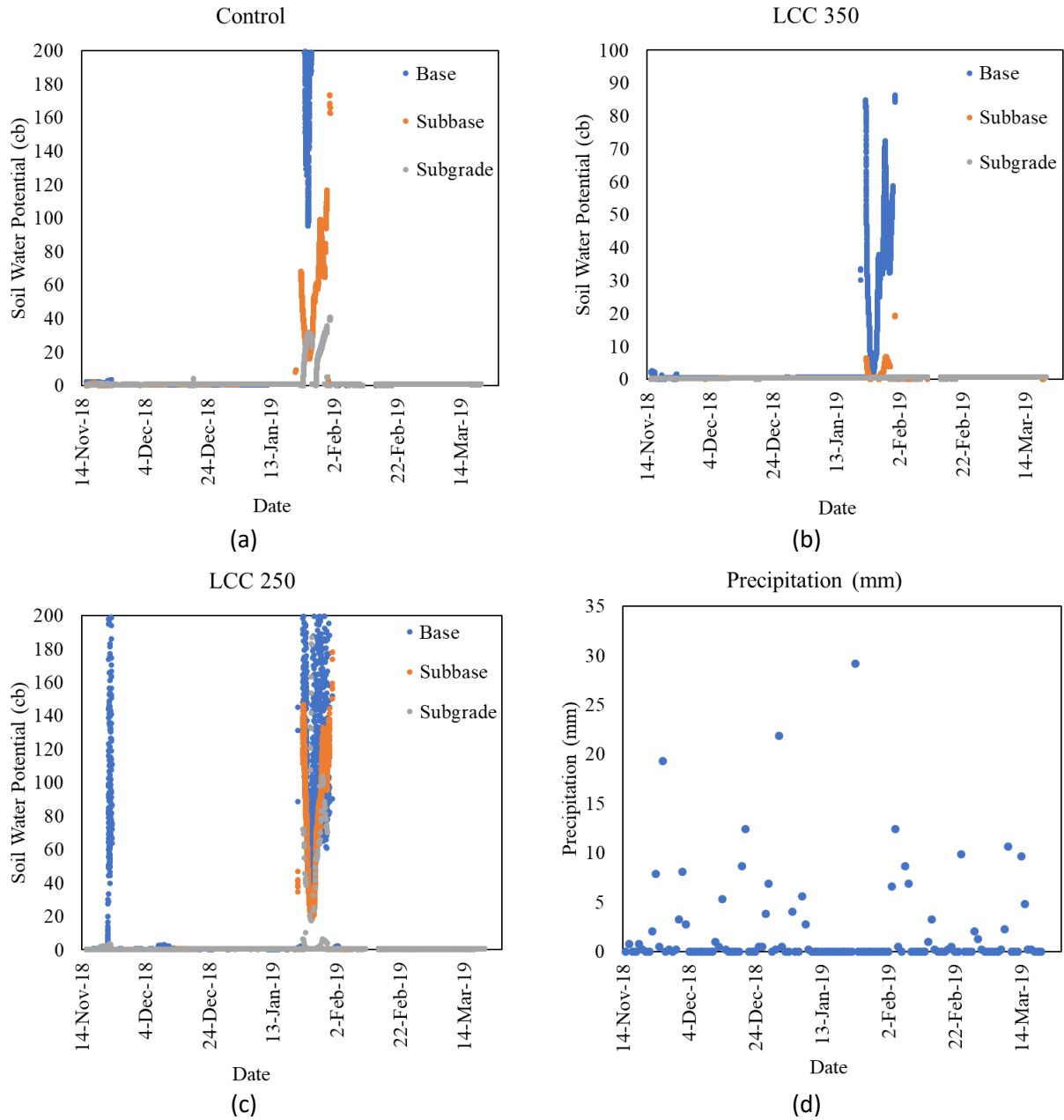


Figure 5: Moisture sensor and precipitation data

Generally, higher temperatures are observed within and below the subbase layer for the LCC section compared with the control section. This depicts that the LCC material could have good insulation properties.

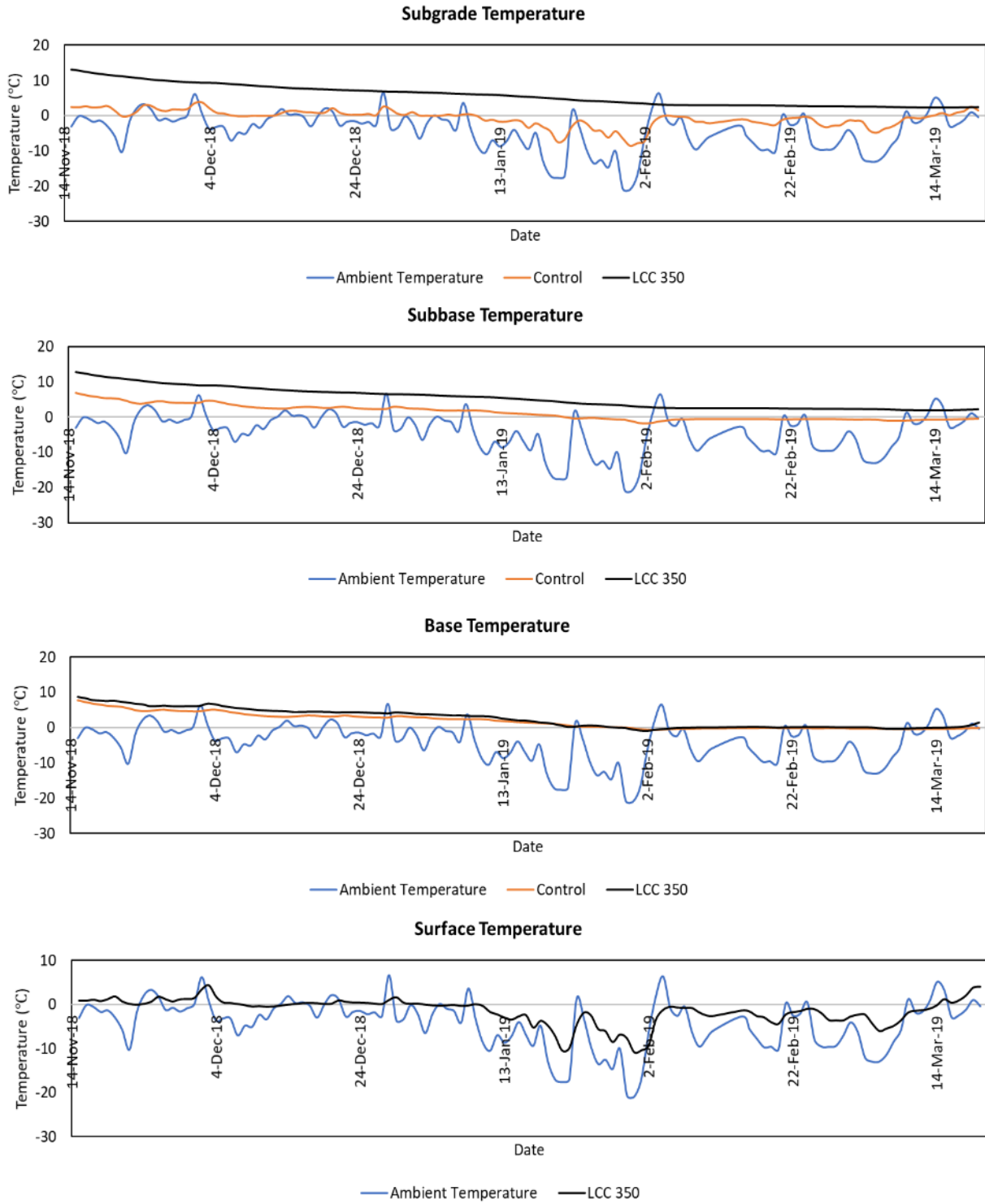


Figure 6: Temperature within the pavement

Table 2: R² values for relationship of ambient and pavement layer temperature

Pavement Layer	Subgrade	Subbase	Base	Surface
Control	0.65	0.14	0.12	0.61
LCC 350	0.14	0.11	0.16	

4.3 Earth Pressure Cells

Results of pressure levels obtained from the sensors compared with average subgrade temperatures are presented in Figures 7 and 8. The readings indicate a change in pressure from the first readings recorded. Some peak pressure points, especially for the LCC 350 section, were found to correspond with bus schedule times at the location. In order to observe the effect of temperature on pressure levels, regression analysis was performed between ambient temperatures and pressure levels. Results showed a slight correlation with pressure values in the control section ($R^2=0.44$) but less with the LCC 350 section ($R^2=0.11$). The temperature values from the LCC 350 subgrade sensor was used to compare pressure for the LCC 250 and results displayed an R^2 of 0.62. This could be as a result of the temperature used which was not measured directly from the layer, or the fact that the pavement thickness is lower compared with the other sections.

The pressure trend showed that relatively high temperatures did not have an effect on pressure levels for the LCC and control sections, however, when temperatures became significantly lower (-10°C subgrade temperature with -25°C ambient temperature), as observed in January of 2019 for the control section, the pressure levels increased significantly up to -19KPa . However, since temperature levels in the LCC subgrade layer did not significantly drop, pressure levels appeared not to be influenced by the low ambient temperatures.

Generally, pressure levels in the control section seemed higher than the LCC sections, especially in very low temperatures. The LCC 250 section appeared to have more pressure induced on the subgrade than the LCC 350 section. This could be a resultant effect of the lower subbase layer thickness of the 250 section compared to the 350 section.

4.4 Strain Gauges

Figure 9 displays the strain measurements recorded. The readings imply the change in strain levels from the initial readings documented. As the record time interval is set to five minutes, traffic loads are generally not directly on top of the strain gauges when it records. The strain readings in the asphalt layer showed tension and compression response in the LCC 350 section; however, the response in the control section was found to be minimal, this could be due to the absence of traffic on the gauges. Transverse strain readings at the middle of the LCC 350 section gave positive values which represent the tensile strain. However, the longitudinal strain in the same location showed both positive and negative values. This denotes that both compressive and tensile strain occurred. The transverse strain readings at the bottom of the LCC 350 section slightly increased over time in tensile strain, but, the longitudinal strain readings showed mostly negative values which indicate compression.

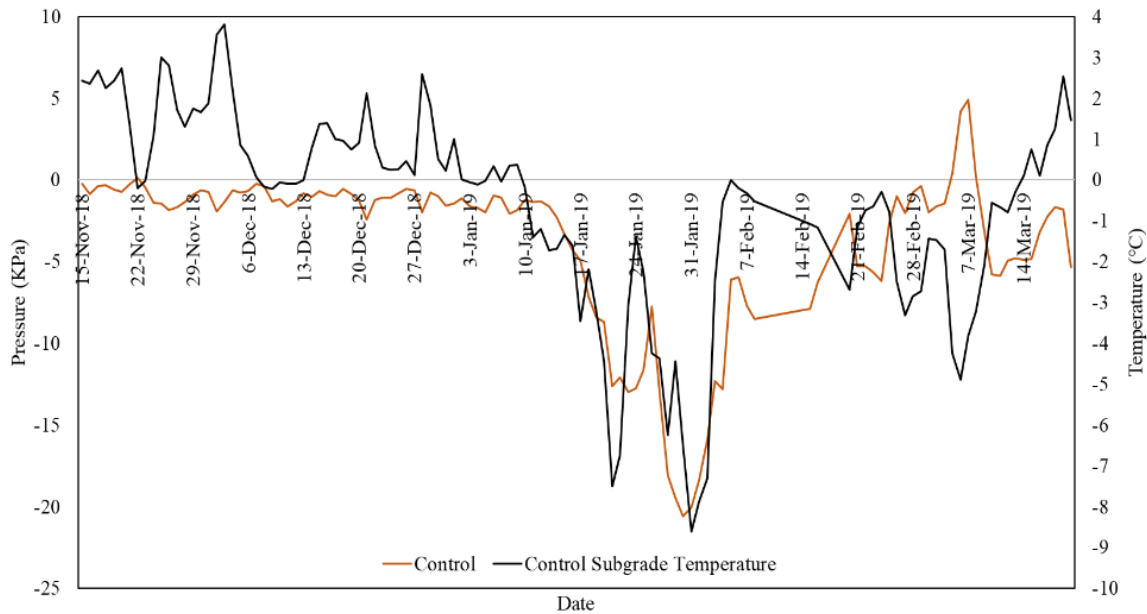


Figure 7: Pressure readings for control section

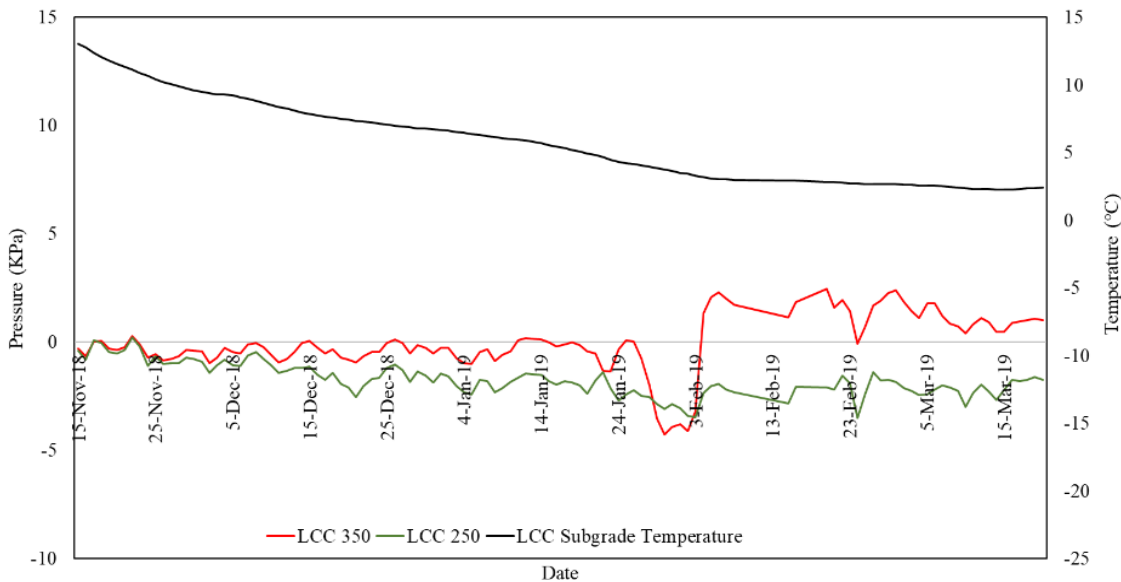


Figure 8: Pressure readings for LCC 350 and 250

Transverse strain readings in the middle of the LCC 250 section demonstrated both compression and tension. This is expected since it is in the middle of the layer with a lower thickness than the LCC 350 section. However, longitudinal strain readings at the same location showed mostly tensile strain. Transverse strain readings at the bottom of the LCC 250 section depicted similar trends as that in the LCC 350 section. As the LCC layer could be seen as a beam, the bending of the layer caused by traffic load could generate compression at the upper part and tension at the

bottom part of the LCC layer. This explains why there are tension and compression near the middle of the layer and more tensile strain at the bottom of the LCC layer in the transverse direction. It is also possible that strain levels are influenced by temperature as previous research has observed (Kodippily et al., 2018); thus, further analysis is required to assess this relationship. Intermittently, some of the strain gauges did not record at all; this explains the gap in the data points.

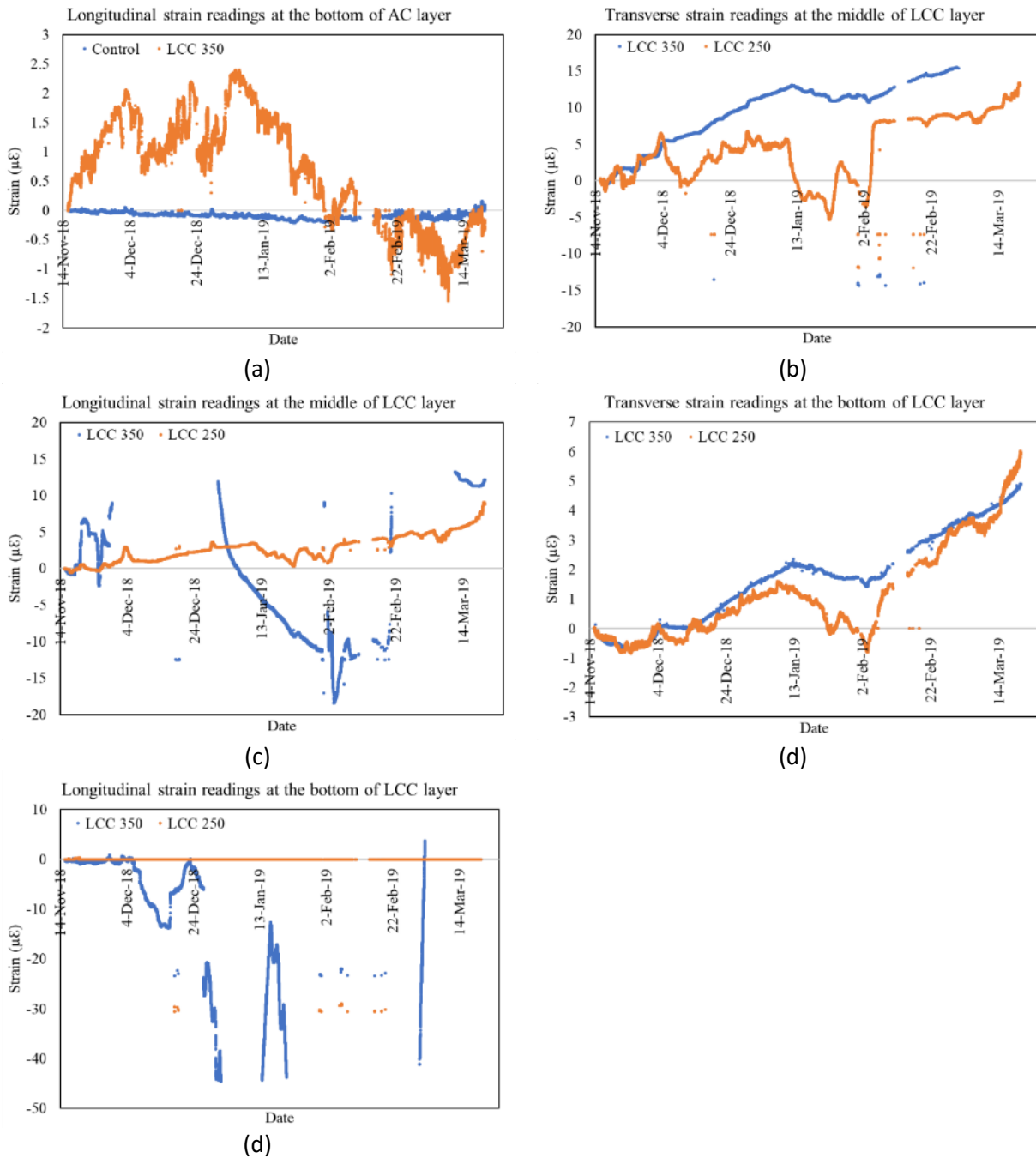


Figure 9: Strain gauge data

Also, four strain gauges in the surface layer have been excluded from the analysis because they either gave minimal intermittent readings or no readings at all. To better understand the strain readings, further monitoring of the data output is required. Besides, a static load test is planned for this trial section to monitor actual responses of the strain gauges.

4.5 Concrete maturity meter

The temperature trend within the installed LCC layers for the first twenty-eight days is presented in Figure 10. It is observed that heat of hydration peaked within the LCC 350 and 250 subbase layers at 55°C and 46°C respectively about twelve hours after casting. This indicates that the LCC had a setting time of about twelve hours. Temperature increase within the LCC 350 and 250 was also noted after the placing of asphalt concrete with LCC temperatures increasing and reaching another peak at about twenty-four hours after the asphalt concrete paving operation time.

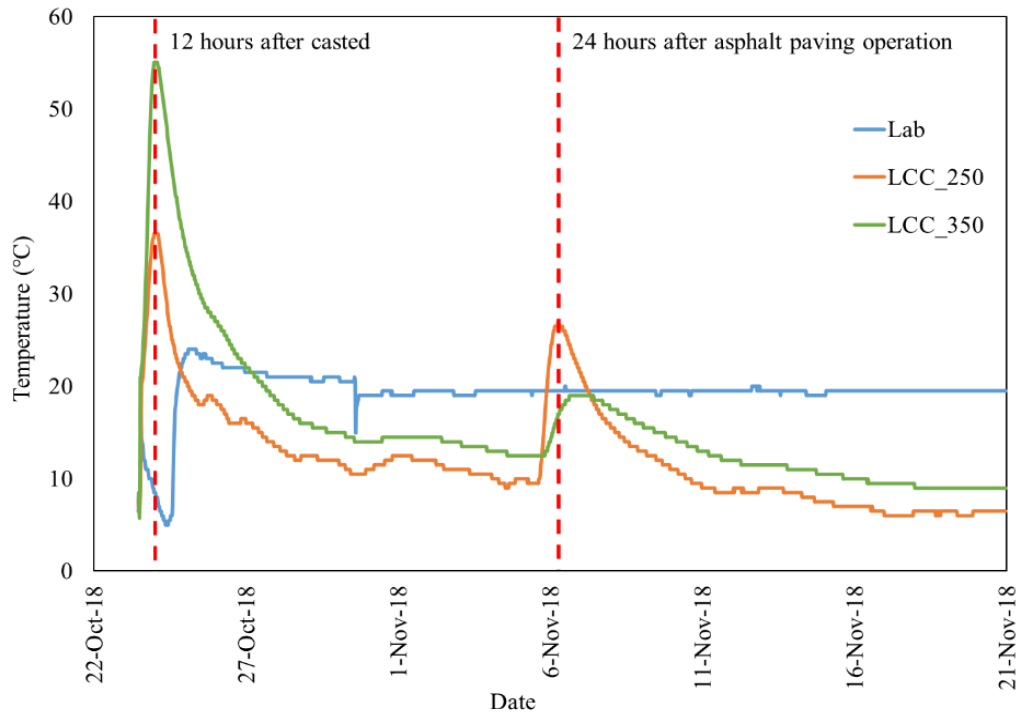


Figure 10: Twenty-eight days temperature profile of LCC

The logged temperature from the sensor installed in the specimen was correlated with compressive strength result obtained from the laboratory. Figure 11 shows the compressive strength gain over twenty-eight days with 28-day compressive strength of 1.67MPa. This strength is greater than the 0.5 MPa typically required for subbase material in Ontario (Maher and Logan, 2016). The interval plot shows 95% upper and lower limit from the mean with each day's standard deviation used to calculate these intervals. The LCC maturity curve was determined based on the strength and Temperature-Time Factor (TTF) using the Nurse-Saul method with a datum temperature of -10°C. This is the typical temperature for regular concrete and method followed is in accordance with ASTM C 1074. The hyperbolic curve fit model was used. An illustration of the maturity curve for the LCC 250 section is presented in Figure 12. The ultimate strengths for the LCC 350 section

were found to be 2.14 MPa, the LCC 250 was 2.02MPa, and for the lab specimen was 1.92MPa. This indicates that LCC thickness and curing method could affect its ultimate strength gain over time.

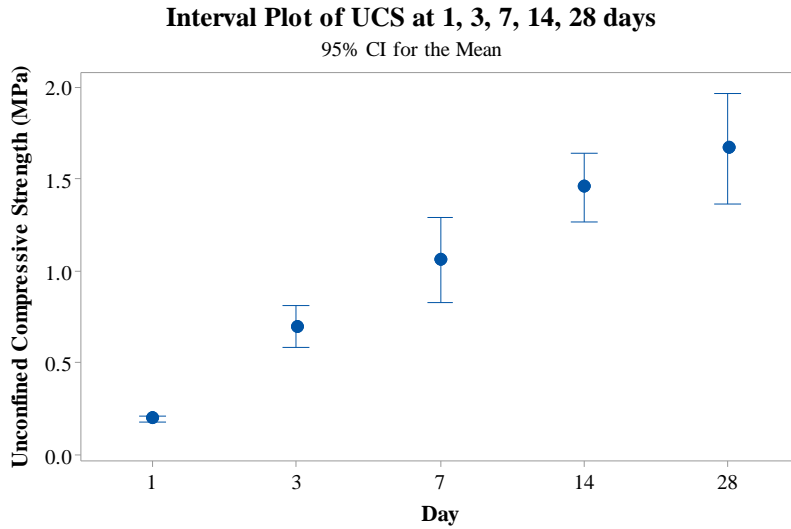


Figure 11: LCC average compressive strength

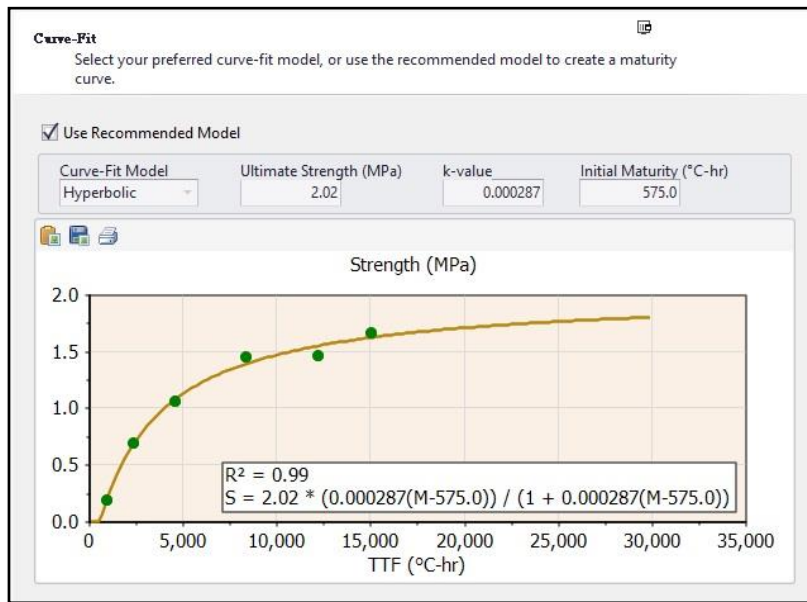


Figure 12: Maturity Curve for 250mm LCC section

5.0 Conclusions and Recommendations

This study was conducted to describe the instrumentation installation and examine and compare preliminary field performance of using Lightweight Cellular Concrete or Granular B as subbase material in a pavement structure. A trial section was constructed in the Region of Waterloo with

instrumentation installed within the pavement to monitor pavement responses using LCC and Granular B material typically used in Canada. The instrumentation included a total of three earth pressure cells, fourteen strain gauges, two concrete maturity meters, three thermistor strings and a weather station consisting of a rain gauge, solar radiation shield, and a temperature data logger. The sensors have been monitored since November 15th, 2018 and this process is ongoing.

Preliminary results indicate that the 475Kg/m³ density LCC has adequate 28-day compressive strength of 1.67MPa, which is more than three times higher than the requirement in Ontario to support the pavement structure as subbase layer, making it a potential alternative. LCC has a typical setting period of twelve hours with its ultimate strength possibly reaching or exceeding 2.20MPa depending on LCC thickness and curing method. LCC could be potentially beneficial as an insulating layer in the pavement structure as temperatures within and below LCC layers were an average of 5°C and 7°C higher than temperatures within and below the Granular B layer respectively. Generally, this temperature difference between the LCC and Granular B sections ranged from 2 to 7°C for the subbase and, 6 to 14°C for subgrade layers. Temperatures within and below the LCC layers remained above 0°C even when ambient temperatures were well below freezing. This was not the case for the Granular B layer and layers beneath. This means that the LCC could potentially reduce the freeze-thaw cycle within the pavement structure, hence reducing damage due to freeze-thaw. Pavement surface temperature was comparable to ambient temperatures; however, the trend differed for the lower layers. Conversely, the subgrade temperature beneath the Granular B layer appeared to be influenced by ambient temperature. This could be as the result of moisture content and groundwater level.

LCC could also potentially reduce pressure levels experienced on the pavement subgrade compared to Granular B, as very low temperatures could significantly increase pressure levels on the subgrade beneath Granular B material compared with LCC material. Although, higher temperature seemed to have less impact on pressure levels. Pressure levels were higher beneath Granular B layer than LCC layer. LCC thickness could likewise be a factor affecting subgrade pressure levels, as higher thickness could reduce pressure levels. This was observed comparing the LCC 250 and 350 sections.

Moisture data indicates that most layers were saturated with water throughout the study period. However, the base layer for all sections indicated lower water levels for some days in late-January. This could be due to the melting of frozen water within the layer and its draining away from the base layer. For better understanding of the moisture characteristics for each section, more data periods in varying weather conditions is necessary. Strain levels within the LCC reduce with increases in layer thickness. The middle of the LCC layer appeared to experience tensile and compressive strain, but the bottom mostly experienced tension, especially with greater layer thickness. Beneath the asphalt layer, a greater fluctuation and magnitude in strain levels are noted for the LCC section, while the control section experienced a minimal change in strain levels, likely due to the absence of traffic loads on the control section.

Three strain gauges were found to give no readings, with another one providing intermittent readings. One thermistor string has been excluded from analysis due to technical challenges of reading the data; otherwise, other sensors have been observed to be functional. Since instrumentation is prone to damage, during and even after installation, it is advisable to

incorporate as many as possible to obtain reasonable data from them. Also, data should continually be monitored over a longer period, to enable an assessment of the trend in various measurement across varying weather conditions. Longer data periods are very important when performing these kinds of analysis. In addition, it would be necessary to perform a static load test on this trial section to monitor actual responses of the strain gauges and pressures cells, before detailed analysis can be performed. Further analysis is required to assess the relationship between strain levels within the pavement structure and temperature

6.0 References

Arulajah A, Disfani M.M, Maghool F., and Du Y.J. 2015. "Engineering and environmental properties of foamed recycled glass as a Lightweight engineering material." *Journal of cleaner production*, 96, pp. 369-375.

Campbell Scientific. 2005. Operators Manual: CR1000 measurement and control system. Revision February 2018. https://s.campbellsci.com/documents/ca/manuals/cr1000_man.pdf

Dolton B., Witchard M., Luzzi D., and Smith T.J. 2016. "Application of lightweight cellular concrete to reconstruction of settlement prone roadways in Victoria." Paper presented at the GEOVANCOUVER 2016.

El-Hakim M. Y. 2009. Instrumentation and Overall Evaluation of Perpetual and Conventional Flexible Pavement Designs. A thesis presented to the University of Waterloo in fulfillment of the thesis requirement for the degree of Doctor of Philosophy in Civil Engineering.

Henderson V. 2012. Evaluation of the Performance of Pervious Concrete Pavement in the Canadian Climate. A thesis presented to the University of Waterloo in fulfillment of the thesis requirement for the degree of Doctor of Philosophy in Civil Engineering.

Hoff Inge, Watn A, Oiseth E, EMDAL A., and Amundsgard, K O. 2002. "Light Weight Aggregate (LWA) Used In Road Pavements." *Proceedings of the 6th international conference on the bearing capacity of roads and airfields*, Lisbon, Portugal, 2, pp. 1013-22.

Kodippily, S., Yeaman, J., Henning, T., and Tighe, S. 2018. "Effects of extreme climatic conditions on pavement response." *Road Materials and Pavement Design*. DOI: 10.1080/14680629.2018.1552620

Maher, M. L. J. and Hagan, J. B. 2016. "Constructability benefits of the use of lightweight foamed concrete fill (Ifcf) in pavement applications." *Canadian Society for Civil Engineering Annual Conference 2016: Resilient Infrastructure*, 2, pp. 1354–1362.

Mallick, R. B. and El-Korchi, T. 2017. *Pavement Engineering: Principles and Practice*. CRC Press.

MTO. 2014. *Ontario Traffic Manual –Book 7: Temporary Conditions*. St. Catherines, ON: Ministry of Transportation of Ontario.

Perera, R. W., and Elkins, G. E. 2015. *LTPP Manual for Profile Measurements and Processing*. Federal Highway Administration McLean, Virginia.

Pickel, D. J., Tighe, S. L., Lee, W., and Fung, R. 2018. "Highway 400 Precast Concrete Inlay Panel Project: Instrumentation Plan, Installation, and Preliminary Results." *Proceedings of Transportation Research Board 97th Annual Meeting*. Washington D.C., United States: